

The mouse ortholog of NEIL3 is a functional DNA glycosylase in vitro and in vivo

Minmin Liu^a, Viswanath Bandaru^a, Jeffrey P. Bond^a, Pawel Jaruga^{b,c}, Xiaobei Zhao^d, Plamen P. Christov^e, Cynthia J. Burrows^d, Carmelo J. Rizzo^e, Miral Dizdaroglu^b, and Susan S. Wallace^{a,1}

^aDepartment of Microbiology and Molecular Genetics, The Markey Center for Molecular Genetics, University of Vermont, Stafford Hall, 95 Carrigan Drive, Burlington, VT 05405-0086; ^bChemical Science and Technology Laboratory, National Institute of Standards and Technology, Building 227/A243, Gaithersburg, MD 20899; ^cDepartment of Clinical Biochemistry, Collegium Medicum, Nicolaus Copernicus University, Bydgoszcz, Poland; ^dDepartment of Chemistry, University of Utah, Salt Lake City, UT 84112-0850; and ^eDepartments of Chemistry and Biochemistry and Center in Molecular Toxicology, Vanderbilt University, Nashville, TN 37235-1822

Edited* by Philip C. Hanawalt, Stanford University, Stanford, CA, and approved January 21, 2010 (received for review July 30, 2009)

To protect cells from oxidative DNA damage and mutagenesis, organisms possess multiple glycosylases to recognize the damaged bases and to initiate the Base Excision Repair pathway. Three DNA glycosylases have been identified in mammals that are homologous to the *Escherichia coli* Fpg and Nei proteins, Neil1, Neil2, and Neil3. Neil1 and Neil2 in human and mouse have been well characterized while the properties of the Neil3 protein remain to be elucidated. In this study, we report the characterization of *Mus musculus* (house mouse) Neil3 (MmuNeil3) as an active DNA glycosylase both in vitro and in vivo. In duplex DNA, MmuNeil3 recognizes the oxidized purines, spiroiminodihydantoin (Sp), guanidinohydantoin (Gh), 2,6-diamino-4-hydroxy-5-formamidopyrimidine (FapyG) and 4,6-diamino-5-formamidopyrimidine (FapyA), but not 8-oxo-7,8-dihydroguanine (8-oxoG). Interestingly, MmuNeil3 prefers lesions in single-stranded DNA and in bubble structures. In contrast to other members of the family that use the N-terminal proline as the nucleophile, MmuNeil3 forms a Schiff base intermediate via its N-terminal valine. We expressed the glycosylase domain of MmuNeil3 (MmuNeil3 Δ 324) in an *Escherichia coli* triple mutant lacking Fpg, Nei, and MutY glycosylase activities and showed that MmuNeil3 greatly reduced both the spontaneous mutation frequency and the level of FapyG in the DNA, suggesting that Neil3 plays a role in repairing FapyG in vivo.

base excision repair | endonuclease VIII Like 3 | 2,6-diamino-4-hydroxy-5-formamidopyrimidine (FapyG) | Spiroiminodihydantoin

DNA glycosylases play an important role in maintaining genomic integrity by recognizing various nonhelix distorting base lesions created by ionizing radiation, alkylating, or oxidizing agents, which are often cytotoxic or mutagenic (1). DNA glycosylases cleave the N-glycosylic bond and release the base lesion from the sugar backbone, resulting in an apurinic or apyrimidinic (AP) site (2). Besides glycosylase activity, some of these enzymes also have a lyase activity to process the AP site. In this way, DNA glycosylases initiate the Base Excision Repair (BER)[†] pathway and create the substrates for further processing by a series of BER enzymes including phosphodiesterases, AP endonucleases, DNA polymerases, and DNA ligases to complete lesion repair (3).

DNA glycosylases that recognize oxidized bases can be divided into two families based on structure and sequence homology (4, 5), the Nth family, whose members are widely distributed in bacteria, archaea, and eukaryotes (5), and the Fpg/Nei family, which is more sparsely distributed across phyla. Fpg/Nei family members are characterized by a signature helix-two turns-helix (H2TH) motif and a zinc finger (or “zincless finger”) motif for DNA binding; they also have a conserved N terminus harboring a proline residue (P2) important for catalysis (6). In *Escherichia coli*, formamidopyrimidine DNA glycosylase (EcoFpg) mainly recognizes oxidized purines (7), and endonuclease VIII (EcoNei) mainly recognizes oxidized pyrimidines and adenine-derived 4,6-diamino-5-formamidopyrimidine (FapyA) (8).

A number of years ago, three Fpg/Nei homologs were identified in mammals, Neil1, Neil2, and Neil3 (9–13). Neil1 and Neil2 have been successfully characterized and their substrate specificities well studied (9–13). However, unlike Neil1 and Neil2, Neil3 has a long C-terminal extension with unique structural features (summarized in Fig. 1A) and unknown function. Neil3 also lacks the catalytic proline at its N terminus, but has instead a valine residue. Although the N-terminal valine is present in another Fpg/Nei family member from *Acanthamoeba polyphaga* mimivirus (MvNei2) which has robust glycosylase activity (14), there is no direct evidence so far that this residue functions in catalysis. Therefore, it was difficult to predict if Neil3 actually had glycosylase activity.

Several attempts to verify the glycosylase activity of Neil3 proteins have been unsuccessful. Although Morland et al. (12) found that lysates from insect cells overexpressing human NEIL3 can recognize 2,6-diamino-4-hydroxy-5N-methylformamidopyrimidine (MeFapyG) in vitro, subsequent studies failed to detect any glycosylase activity of NEIL3 using either the purified or the in vitro translated full-length NEIL3 or its glycosylase domain (15–17). In addition, Torisu et al. generated Neil3 knock-out mice, however, these mice were viable and remained apparently healthy into adulthood (24 weeks) with no overt phenotype (17). Notably, Takao et al. were able to detect weak lyase activity for a single-stranded substrate using the purified NEIL3 glycosylase domain. They also observed that expression of NEIL3 partially rescued the hydrogen peroxide sensitivity phenotype in an *E. coli nth nei* mutant (18). Still, whether Neil3 contained glycosylase activity remained controversial. In this paper, we report the characterization of *Mus musculus* (house mouse) Neil3 (MmuNeil3) as a functional glycosylase using purified full-length MmuNeil3 (MmuNeil3 wt) and its glycosylase domain (MmuNeil3 Δ 324). Moreover, by utilizing an *E. coli* mutation frequency assay, we were able to demonstrate the in vivo glycosylase activity of MmuNeil3.

Author contributions: M.L., V.B., J.P.B., M.D., and S.S.W. designed research; M.L. and P.J. performed research; X.Z., P.P.C., C.J.B., and C.J.R. contributed new reagents/analytic tools; M.L., J.P.B., M.D., and S.S.W. analyzed data; M.L. and S.S.W. wrote the paper.

The authors declare no conflict of interest.

*This Direct Submission article had a prearranged editor.

[†]ABBREVIATIONS BER, Base Excision Repair; Fpg, formamidopyrimidine DNA glycosylase; Nei, endonuclease VIII; Nth, endonuclease III; 8-oxoG, 8-oxo-7,8-dihydroguanine; 8-oxoA, 7,8-dihydro-8-oxoadenine; FapyG, 2,6-diamino-4-hydroxy-5-formamidopyrimidine; FapyA, 4,6-diamino-5-formamidopyrimidine; MeFapyG, 2,6-diamino-4-hydroxy-5N-methylformamidopyrimidine; Sp, Spiroiminodihydantoin; Gh, Guanidinohydantoin; Tg, thymine glycol; 5-OHC, 5-hydroxycytosine; 5-OHU, 5-hydroxyuracil; 5OHMH, 5-hydroxy-5-methylhydantoin; DHT, 5,6-dihydrothymine; DHU, 5,6-dihydrouracil; AP, apurinic or apyrimidinic site;

¹To whom correspondence should be addressed. E-mail: susan.wallace@uvm.edu.

This article contains supporting information online at www.pnas.org/cgi/content/full/0908307107/DCSupplemental.

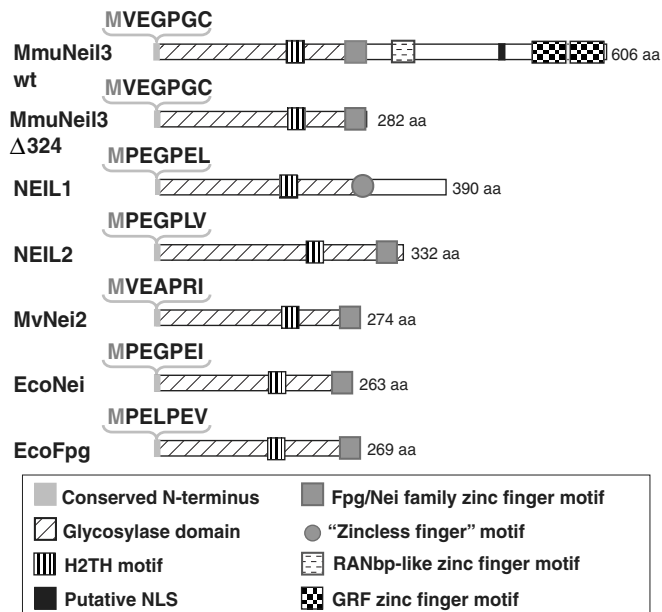


Fig. 1. Alignment of the structural features of *Mus musculus* Neil3 with representative members of the Fpg/Nei family. Domains and motifs in the scheme are described in the box below. Sequences of the conserved N terminus are shown in the bracket. MmuNeil3 wt: wild-type *Mus musculus* Neil3; MmuNeil3Δ324: glycosylase domain of *Mus musculus* Neil3; NEIL1: human Neil1; NEIL2: human Neil2; MvNei2: Mimivirus Neil2; EcoNei: *Escherichia coli* Nei; EcoFpg: *Escherichia coli* Fpg.

Results and Discussion

MmuNeil3 Constructs. In order to study the substrate specificity of MmuNeil3, we first cloned and expressed the wild-type full-length MmuNeil3 with a C-terminal His tag (MmuNeil3 wt) in *E. coli*. Considering MmuNeil3 wt was unstable and prone to aggregate during the purification process, we were only able to partially purify the protein. We therefore constructed a C-terminal 324 amino acid truncation mutant of MmuNeil3 (MmuNeil3Δ324) fused with a C-terminal His tag. Like other Fpg/Nei family members, MmuNeil3Δ324 possesses the complete Fpg/Nei-like glycosylase domain that contains a conserved N terminus, the H2TH motif, and the Fpg/Nei family zinc finger motif (Fig. 1). MmuNeil3Δ324 was more stable than the wild-type protein and we were able to overexpress and purify Mmu-

Neil3Δ324 to apparent homogeneity. We then examined the proper processing of the N-terminal initiator methionine residue in our protein preparations because it might mask the potential active site in MmuNeil3. By Edman degradation N-terminal sequencing we estimated that about 46.4% of MmuNeil3 wt and 57.9% of MmuNeil3Δ324 had the N-terminal Met processed and verified the N-terminal sequences of both protein constructs (Table S1).

MmuNeil3 is a Bifunctional DNA Glycosylase That Recognizes Sp and Gh in Double-Stranded Substrates. We tested DNA glycosylase/AP lyase activity of both MmuNeil3 wt and MmuNeil3Δ324 on double-stranded DNA substrates containing a single modified base. As shown in Fig. 2, MmuNeil3 wt and MmuNeil3Δ324 are bifunctional with both glycosylase and lyase activities. The best substrates for both proteins are the further oxidation products of 8-oxoG, Sp (includes two diastereomers Sp1 and Sp2) and Gh (Figs. 2 and 3A). MmuNeil3 wt and MmuNeil3Δ324 showed weaker activity on MeFapyG and some pyrimidine lesions such as Tg and 5-OHU, but no activity on 8-oxoG (Fig. 3A and Fig. S1). Unlike EcoFpg, EcoNei, and NEIL1 that cleave their substrates via β,δ-elimination leaving the majority of cleavage products with a phosphate at the 3' end (9, 11), but like MvNei2 (14), MmuNeil3 wt, and MmuNeil3Δ324 cleaved their substrates primarily via β-elimination leaving cleavage products with an α,β-unsaturated aldehyde (Fig. 2). Although small amounts of β,δ-elimination products were observed.

MmuNeil3 Prefers Single-Stranded, Fork and Bubble Substrates. Because NEIL1 and NEIL2 recognize lesions in single-stranded, fork and bubble structured substrates (19, 20), we asked whether MmuNeil3 can also recognize lesions in these substrates. When tested on ³²P-labeled single-stranded oligodeoxynucleotides containing various base lesions, interestingly, MmuNeil3 wt and MmuNeil3Δ324 were active on most of these lesions (Fig. 3B and Fig. S2). In addition, MmuNeil3 wt and MmuNeil3Δ324 preferred single-stranded substrates over double-stranded substrates measured under the same reaction conditions (Fig. 3, compare B to A). We then examined the activity of MmuNeil3 on 5-OHU carried in forked, single-stranded, double-stranded, or 5-nt, 11-nt and 19-nt bubble structure substrates, and found that MmuNeil3 wt and MmuNeil3Δ324 preferred single-stranded and larger bubble (11-nt and 19-nt bubble) structures over double-stranded, fork, or smaller bubble (5-nt bubble) substrates (Fig. S3). This pattern of substrate preference of MmuNeil3 is similar to NEIL2 that prefers 5-OHU in single-stranded

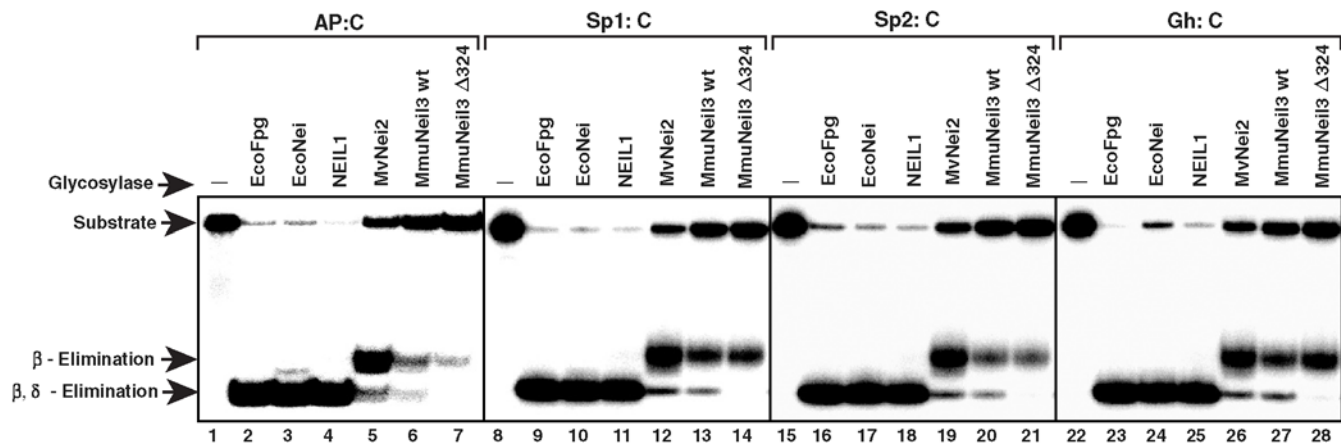


Fig. 2. DNA glycosylase/lyase activity of MmuNeil3. Double-stranded substrates containing Sp1, Sp2, Gh, or an AP site (25 nM) were incubated with 25 nM active MmuNeil3 wt (lanes 6, 13, 20, and 27), MmuNeil3Δ324 (lanes 7, 14, 21, and 28), EcoFpg (lanes 2, 9, 16, and 23), EcoNei (lanes 3, 10, 17, and 24), NEIL1 (lanes 4, 11, 18, and 25) and MvNei2 (lanes 5, 12, 19, and 26) at 37 °C for 30 min. Reactions were stopped by formamide stop buffer to measure glycosylase plus lyase activities. Lanes 1, 8, 15, and 22, No enzyme control.

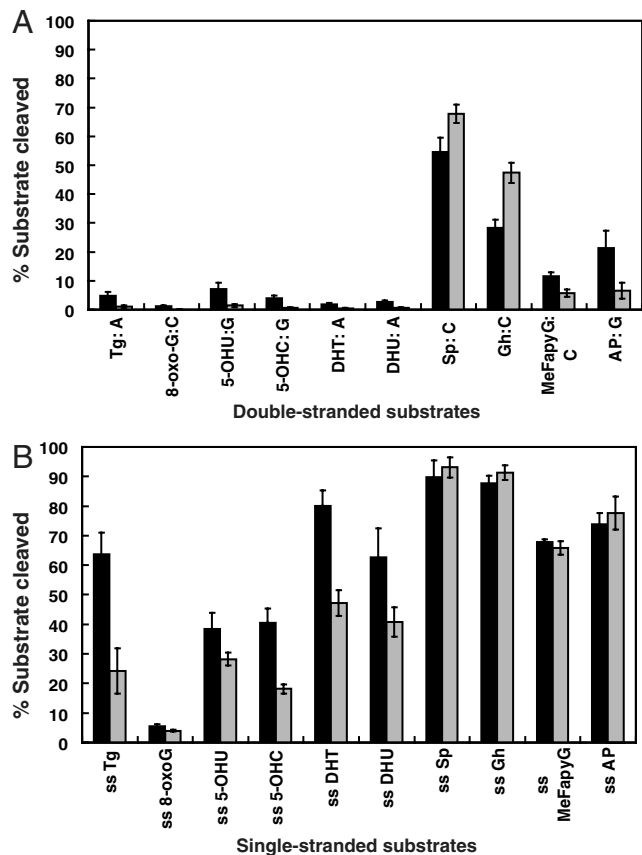


Fig. 3. Quantification of base lesions recognized by MmuNeil3 in (A) double-stranded substrates and (B) single-stranded substrates. 25 nM active MmuNeil3 wt (black) or MmuNeil3Δ324 (gray) was incubated with 25 nM substrate at 37 °C for 30 min. Reactions were stopped by formamide stop buffer to measure glycosylase plus lyase activities. Sp stands for the mixture of Sp1 and Sp2. Data are expressed as means of three independent measurements. Uncertainties are standard deviations.

substrates, fork, and larger bubble substrates, while it differs from EcoNei and NEIL1 that prefer 5-OHU in double-stranded substrates (Fig. S3).

In γ -Irradiated DNA, MmuNeil3 Exhibits a Broad Lesion Recognition Spectrum and Preference for FapyG and FapyA. Because substrate specificity (k_{cat}/K_m) is affected by both k_{cat} and K_m parameters, it is hard to compare the specificity using a single enzyme and substrate concentration at a single time point. We therefore used

a “pooled assay” in which gas chromatography/mass spectrometry (GC/MS) was used to detect the lesions released by a glycosylase from γ -irradiated calf thymus DNA containing multiple lesions. This method allows the measurement of substrate specificity under conditions where the enzyme concentration is far less than the substrate concentration and the enzyme encounters numerous lesions on the same substrate (21). In addition, by normalizing the signals for all substrates recognized by a given glycosylase, we can compare the substrate recognition patterns of different glycosylases (21). Interestingly, MmuNeil3Δ324 exhibits a broad lesion recognition pattern and prefers FapyA and FapyG followed by 5-OHU, 5-OHC, and 5OHMH, then by Tg and 8-oxoA. As with oligodeoxynucleotides containing a single 8-oxoG, no activity on 8-oxoG was detected (Fig. 4). The substrate recognition pattern of MmuNeil3 differs from that of EcoFpg which recognizes oxidized pyrimidines poorly, EcoNei which recognizes FapyA but not 8-oxoA and FapyG, and from NEIL1 which prefers FapyA and FapyG and shows weak preference for oxidized pyrimidines (Fig. 4, Table S2).

Kinetics Analysis of MmuNeil3Δ324. We determined the kinetic parameters of MmuNeil3Δ324 with double and single-stranded oligodeoxynucleotides containing an Sp1 or an AP site. The glycosylase activity against Sp1 was analyzed by quenching the reactions with NaOH and heat treatment while the lyase activity was evaluated by quenching with formamide stop buffer. As shown in Table 1, the MmuNeil3Δ324 glycosylase reaction is rapid relative to the lyase reaction; the catalytic turnover rate (k_{obs}) for the glycosylase reaction relative to the rate for the lyase reaction is about 70-fold faster on a double-stranded substrate and 2,000-fold faster on a single-stranded substrate. A time course of MmuNeil3Δ324 excising double-stranded Sp1 under multiple turnover conditions (Fig. S4) suggested that although MmuNeil3Δ324 is bifunctional (with rates of $0.119 \pm 0.016 \text{ min}^{-1}$ for single-stranded Sp1 and $0.053 \pm 0.002 \text{ min}^{-1}$ for double-stranded Sp1 substrates), its lyase activity is not coupled to its glycosylase activity, since the slow lyase reaction of MmuNeil3Δ324 does not limit the enzyme turnover of the glycosylase reaction.

MmuNeil3Δ324 has a similar catalytic turnover rate for the glycosylase reaction (3.2 min^{-1} , Table 1) on double-stranded Sp substrate as does *E. coli* Nei ($1.6\text{--}13.0 \text{ min}^{-1}$ (22–24)) and Fpg ($6.0\text{--}34.2 \text{ min}^{-1}$ (22–24)) proteins, although it is much slower than NEIL1 (177 min^{-1} (25)) on the same substrate. However, MmuNeil3Δ324 exhibits a much higher binding affinity to a double-stranded Sp substrate ($K_m = 0.753 \text{ nM}$, Table 1), compared to EcoFpg ($K_m = 25 \text{ nM}$ (24)) and EcoNei ($K_m = 30 \text{ nM}$ (24)). Therefore, the catalytic specificity of MmuNeil3Δ324 on double-stranded Sp ($4.25 \text{ min}^{-1} \text{ nM}^{-1}$, Table 1)

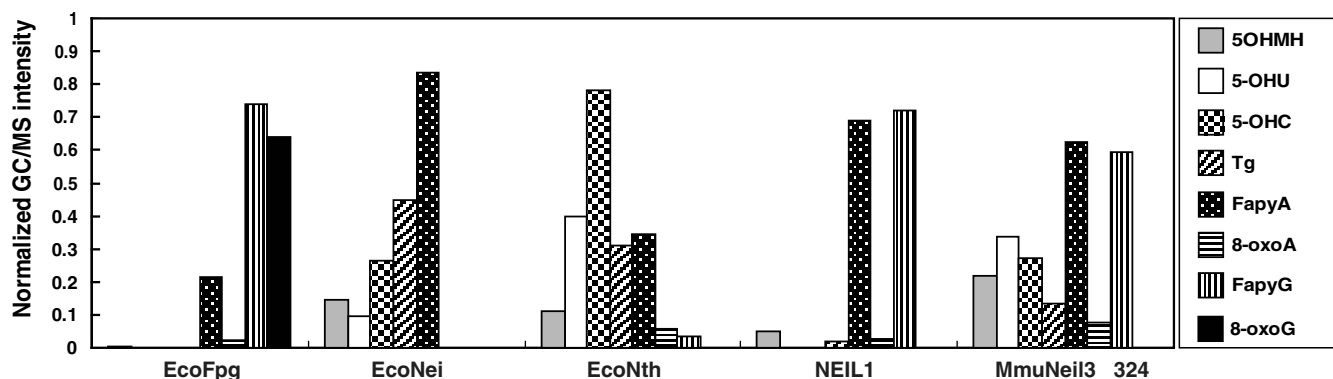


Fig. 4. Substrate specificity of MmuNeil3 on γ -irradiated DNA. The amounts of damaged bases released by each enzyme as measured by GC/MS (Table S2) were normalized to show the preference of each enzyme as described in SI Materials and Methods.

Table 1. Kinetic parameters of MmuNeil3 Δ 324 glycosylase activity. The catalytic turnover rates (k_{obs}) were measured under single turnover conditions as shown in Fig. S4B. The Michaelis constants (K_m) were measured under steady-state conditions as shown in Fig. S4C. Data are expressed as the means of three independent measurements. Uncertainties are standard deviations.

Substrate	k_{obs} (min^{-1})	K_m (nM)	k_{obs}/K_m ($\text{min}^{-1} \text{nM}^{-1}$)
Sp1:C	3.20 ± 0.13	0.753 ± 0.145	4.25 ± 0.84
ss Sp1	184 ± 23	0.331 ± 0.098	556 ± 179
AP: C	0.0468 ± 0.0017	1.52 ± 0.41	0.0308 ± 0.0084
ss AP	0.0927 ± 0.0020	0.452 ± 0.188	0.205 ± 0.085

is comparable to that of EcoFpg ($0.24\text{--}5.05 \text{ min}^{-1} \text{ nM}^{-1}$ (22, 24)), and higher than EcoNei ($0.05\text{--}1.39 \text{ min}^{-1} \text{ nM}^{-1}$ (22, 24)).

Like NEIL1 and NEIL2, MmuNeil3 Δ 324 prefers single-stranded DNA or partially single-stranded DNA structures such as bubble and fork structures (Fig. 3 and Fig. S3). Both NEIL1 and NEIL2 show faster catalytic turnover rates on bubble substrates (0.125 min^{-1} for NEIL1 and 0.038 min^{-1} for NEIL2 (19)) than on the corresponding duplex substrate (0.0658 min^{-1} for NEIL1 and 0.0082 min^{-1} for NEIL2 (19)) with DNA containing 5-OHU, as well as higher specificity (about 3-fold higher for NEIL1 and 7-fold higher for NEIL2 (19)). In contrast, we observed the catalytic turnover rate of MmuNeil3 Δ 324 on single-stranded Sp1 to be about 58 times higher than on a duplex Sp1 substrate while the specificity is about 130-fold higher. Thus, MmuNeil3 Δ 324 appears to be relatively more efficient on single-stranded DNA substrates than either NEIL1 or NEIL2. According to the structural and biophysical studies of many DNA glycosylases bound to duplex substrates, damage specific glycosylases go through a “nucleotide flipping” step to “push” the base lesion out of the helix, “plug in” amino acids to stabilize the opposite strand and “pull” the lesion into the active site pocket (26, 27). It is possible that the single-stranded substrates (Fig. 3B, Fig. S3, and Table 1) and larger bubble structured substrates (Fig. S3) used in our study lowered the transition state energy barrier for MmuNeil3 during this “nucleotide flipping” step in vitro. Whether Neil3 proteins exhibit this single-stranded substrate preference in vivo is still unknown. It is possible that like the NEIL1 and NEIL2 proteins, which have been proposed to function during transcription and/or replication when partly unwound regions of DNA can be accessed (3), Neil3 proteins might also function in single-stranded regions of the genome during these processes. Also there is an interesting observation that NEIL2 can be stimulated by YB-1 protein so that the catalytic turnover rate of NEIL2 increases about 3-fold on a bubble structured substrate containing 5-OHU (28). It is also possible that Neil3 proteins require a partner(s) to stimulate its activity in vitro and in vivo.

MmuNeil3 Forms a Schiff Base via an N-Terminal Valine. To test whether the primary amine of the valine residue in MmuNeil3 forms a transient imine intermediate (Schiff base) for catalysis, we first used a borohydride-dependent “trapping assay” to measure Schiff base formation by MmuNeil3. In this assay, we incubated an equal molar ratio of active enzyme and substrate in the presence of 50 mM NaCNBH₃, which can reduce the transient Schiff base intermediate to a covalent enzyme-DNA complex. Using the ³²P-labeled double or single-stranded substrates containing Gh, we detected the enzyme-DNA complex formed by MmuNeil3 wt (lanes 6, 13 in Fig. 5) and MmuNeil3 Δ 324 (lanes 7, 14 in Fig. 5) migrating at the predicted positions on an SDS-PAGE gel relative to EcoFpg (lanes 2, 9), EcoNei (lanes 3, 10), NEIL1 (lanes 4, 11), and MvNei2 (lanes 5, 12) as controls. We then further tested whether the DNA was linked to the N-terminal valine in the MmuNeil3 Δ 324-DNA complex using Edman degradation. If the DNA was linked to the N-terminal

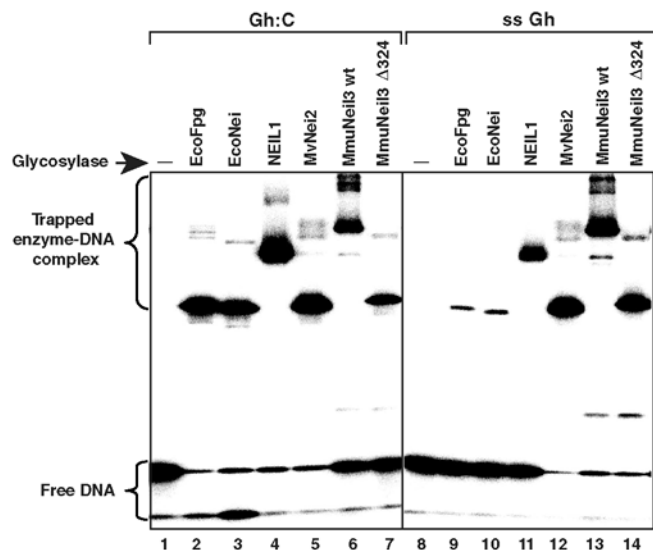


Fig. 5. Schiff base assay of purified MmuNeil3 proteins. Lanes 6 and 13, MmuNeil3 wt; lanes 7 and 14, MmuNeil3 Δ 324. Controls: Lanes 1 and 8, no enzyme control; lanes 2 and 9, trapping with purified EcoFpg; lanes 3 and 10, EcoNei; lanes 4 and 11, NEIL1; lanes 5 and 12, MvNei2.

valine, the MmuNeil3 Δ 324-DNA complex would sequence differently from the MmuNeil3 Δ 324 protein alone, and as predicted, we observed that the first sequencing cycle of the enzyme-DNA complex appeared as a blank cycle (Table S1). Because valine can form a secondary amine after linkage to the DNA molecule, it can be cleaved by Edman sequencing. However the cleaved DNA cannot be detected and a blank cycle results. To provide direct proof, we created a MmuNeil3 Δ 324 V2P mutant which would be resistant to sequencing if linked to DNA at its N terminus. As we predicted, MmuNeil3 Δ 324 V2P-DNA complex was resistant to sequencing up to six cycles (Table S1). We therefore concluded that the N-terminal valine in MmuNeil3 plays the catalytic role in forming the Schiff base intermediate.

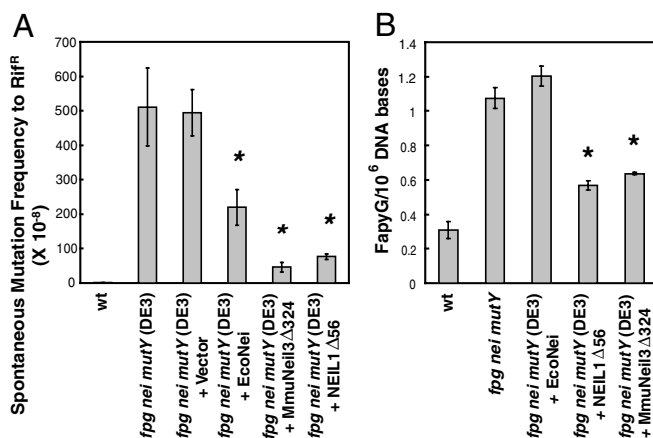


Fig. 6. Substrate specificity of MmuNeil3 in vivo. (A) Spontaneous forward mutation frequencies to rifampin resistance in *E. coli*. Mutants per 10^8 cells are shown. Data are expressed as means of five independent measurements. Uncertainties are standard deviations. Statistical significance was determined by student's *t* test and the *p* values were calculated relative to values in *fpg nei mutY* (DE3) cells; *, *p* < 0.01. (B) GC/MS measurement of the amount of FapyG in *E. coli* genomic DNA. Data are expressed as means of three independent measurements. Uncertainties are standard deviations. The *p* values were calculated relative to values of *fpg nei mutY* triple mutant strain; *, *p* < 0.01.

MmuNeil3 Reduces the Spontaneous Mutation Frequency in an *E. coli* *fpg* *mutY* *nei* Mutant Strain. To test whether MmuNeil3 is active in vivo, we expressed MmuNeil3Δ324 in an *E. coli* *fpg* *nei* *mutY* (DE3) strain, which was derived from the *E. coli* *fpg* *nei* *mutY* strain previously constructed in our laboratory (29), and was designed to express genes under the T7 promoter in the presence of IPTG as an inducer. Because the *E. coli* *fpg* *nei* *mutY* strain exhibits a high Gua to Thy transversion mutation frequency (up to 600-fold higher than the wild-type *E. coli* strain) due to the absence of the glycosylases that protect cells from the mutational effects of guanine-derived lesions, we asked whether the expression of MmuNeil3Δ324 can rescue this phenotype when induced by a low level of IPTG (0.1 mM). We also introduced the empty vector, NEIL1Δ56, and EcoNei into the same strain as controls. We found that the expression of MmuNeil3Δ324 and NEIL1Δ56 significantly reduced the mutation frequency up to 10-fold and 6.4-fold, respectively (Fig. 6A), while the expression of EcoNei reduced the mutation frequency about 2-fold (Fig. 6A). No significant change in the mutation frequency was observed when expressing the empty vector (Fig. 6A). These data suggest that MmuNeil3 recognizes guanine-derived lesions in vivo.

To further probe which guanine-derived lesions were recognized by MmuNeil3 in our *E. coli* mutation frequency assay, we isolated the genomic DNA from the experimental strains and quantified the amounts of FapyG and 8-oxoG using GC/MS method. The amount of FapyG in the *fpg* *nei* *mutY* triple mutant strain was about 3-fold more than that in the wild-type strain (Fig. 6B), due to the loss of the endogenous excision activity of FapyG by EcoFpg in the triple mutant strain. When MmuNeil3Δ324 or NEIL1Δ56 was expressed in the triple mutant strain, we observed a significant reduction in the FapyG level (Fig. 6B). No reduction of FapyG in the DNA was observed in the triple mutant expressing EcoNei which does not recognize FapyG (Fig. 6B). These data suggest that like NEIL1, MmuNeil3 recognizes FapyG in vivo. We observed the amount of 8-oxoG to be about the same (about 2 in 10⁶ of DNA bases) under all experimental conditions. It is possible that substantial amounts of 8-oxoG were produced during the isolation of the genomic DNA that masked the actual amount of 8-oxoG in the cells. It is also possible that under the oxidative growth conditions in the mutant strain unable to process 8-oxoG that the 8-oxoG was further oxidized to form other products such as Sp and Gh. Since MmuNeil3Δ324 does not recognize 8-oxoG-containing oligodeoxynucleotides in vitro (Fig. S5), but has weak activity on MeFapyG-containing oligodeoxynucleotides (Fig. S5), and efficiently excises FapyG, but not 8-oxoG, from γ -irradiated DNA (Fig. 4), we conclude that the reduction of mutation frequency observed in the *fpg* *mutY* *nei* triple mutant is mainly due to the activity of MmuNeil3 on FapyG.

Like 8-oxoG, FapyG appears to be a strong mutagenic lesion. FapyG can be bypassed by Klenow exo⁻, which is comparable to the bypass of 8-oxoG, and Ade was shown to be misincorporated opposite FapyG, resulting in Gua \rightarrow Thy transversion mutations (30). Comparison of the mutagenesis caused by 8-oxoG and FapyG was performed in simian kidney cells (COS-7), and more Gua \rightarrow Thy transversion mutations were caused by FapyG than by 8-oxoG in several sequence contexts (31). However, a recent study showed that in *E. coli*, the mutagenicity of 8-oxoG is greater than that of FapyG (32). It is also possible that the reduced mutagenicity we observed in the triple mutant strain is partially due to the further oxidation product of 8-oxoG, Sp, which gives rise to a combination of Gua \rightarrow Thy and Gua \rightarrow Cyt transversion mutations (33, 34) and can be recognized by MmuNeil3. Sp has been shown to accumulate in Nei deficient *E. coli* cells exposed to chromate which requires Nei for its repair (35). Interestingly, EcoNei was also able to reduce the spontaneous mutation frequency in the triple mutant cells albeit not nearly as much as MmuNeil3 (Fig. 6A). Conversely because Nei does not recognize FapyG

(Fig. 4, Table S2) it does not reduce the amount of FapyG that accumulates in *fpg* *mutY* *nei* mutant cells (Fig. 6B). MmuNeil3 also recognizes urea, another oxidation product of 8-oxoG, which can form Gua \rightarrow Thy transversions (36). It would be interesting to see if MmuNeil3 can recognize other oxidation products of 8-oxoG, such as oxazolone, oxaluric acid, and cyanuric acid, which also cause Gua \rightarrow Thy transversion mutations (37–39).

In summary, we have shown that MmuNeil3 is a functional glycosylase that reduces spontaneous mutation frequency in *E. coli* cells, which implies that Neil3 might serve as a backup glycosylase to protect mammalian cells from the mutagenic effects of oxidative base lesions. In addition, our finding that MmuNeil3 also recognizes lethal lesions such as Tg and mutagenic lesions such as FapyG, 5-OHU, and 5-OHC, together with the fact that Neil3 is expressed principally in hematopoietic tissues, in tissues that harbor stem cells in the brain, in various tumor tissues, and during embryonic development (17, 18, 40–42) suggests that Neil3 function might be required in proliferating cells to remove lethal and mutagenic lesions from the genome.

Materials and Methods

Cloning and Protein Purification. Details of the cloning, expression, and purification of wild-type *Mus musculus* Neil3 (MmuNeil3 wt) and its glycosylase domain (MmuNeil3Δ324) will be published elsewhere. Other glycosylases used as controls in this study are listed in *SI Materials and Methods*. Protein concentration was determined using the Bradford protein assay (BioRad). The fraction of active DNA glycosylase was determined by the Schiff base assay or by the molecular accessibility method of Blaisdell and Wallace (43), and all concentrations of protein used in this study were corrected for the fraction of active molecules in each preparation.

Glycosylase/Lyase Activity Assays. The buffer conditions for glycosylase/lyase activity assays of different enzymes were listed in *SI Materials and Methods*. Concentrations of enzymes and substrates used are listed in each figure legend. To assay for glycosylase and lyase activities, reactions were stopped by adding an equal volume of formamide stop buffer (98% formamide, 10 mM EDTA, 0.1% bromophenol blue and 0.1% xylene cyanol). The reaction products were separated on a 12% weight/volume percent polyacrylamide sequencing gel and quantitated with an isotope imaging system (Molecular Imaging System, BioRad). Details of the kinetic analyses are fully described in *SI Materials and Methods*.

GC/MS Data Analysis. To create base lesions in vitro, calf thymus DNA was γ -irradiated with 40 Gray in N₂O saturated phosphate buffer solution as previously described (21, 44). Then 50 μ g DNA was incubated with 1 μ g glycosylase in 50 mM phosphate buffer (pH 7.4) containing 100 mM KCl, 1 mM EDTA and 0.1 mM DTT at 37 °C for 1 h. The subsequent GC/MS analysis was performed as described (21, 44) and the data were collected from three independent experiments using three independently prepared DNA substrates. Normalization of the data is described in *SI Materials and Methods*. To quantify the amount of FapyG and 8-oxoG in the genomic DNA of *E. coli* KL16 wt, *fpg* *nei* *mutY*, and *fpg* *nei* *mutY* (DE3) strains expressing EcoNei, NEIL1Δ56, and MmuNeil3Δ324, cells were cultured in 250 mL LB medium with 0.1 mM IPTG and appropriate antibiotics at 37 °C with shaking at 250 rpm overnight. Genomic DNA was isolated using the Wizard® Genomic DNA Purification Kit (#A1620, Promega) according to the manufacturer's protocol. FapyG and 8-oxoG were released from DNA by EcoFpg and their amounts were measured by GC/MS as previously described (44, 45).

Schiff Base Assay. To trap the Schiff base intermediates of glycosylases, 25 nM active enzyme was incubated with an equal concentration of substrate in 10 μ L reactions containing 50 mM sodium cyanoborohydride (NaCNBH₃) and in the glycosylase/lyase reaction buffers specified above. Reactions were incubated at 37 °C for 30 min, stopped by adding 10 μ L SDS loading buffer (62.5 mM Tris-HCl pH 6.8, 2% SDS, 10% glycerol, 0.01% bromophenol blue and 50 mM BME), heated at 95 °C for 10 min and then resolved on a 12% SDS-PAGE gel. The Schiff base assay was also used to determine the fraction of active enzyme in each preparation as previously described (43).

Determination of Spontaneous Mutation Frequencies in *E. coli*. Details of the construction of experimental strains are described in *SI Materials and Methods*. Single colonies of the experimental strains were cultured overnight at 37 °C in LB medium with appropriate antibiotic selection and 0.1 mM IPTG

to maintain low levels of protein expression. A 1:50 dilution of the overnight culture in the same medium was grown at 37 °C with shaking at 250 rpm until an OD₅₉₅ of 0.5. The subsequent determination of spontaneous mutation frequencies to rifampin resistance were performed as previously described (29).

ACKNOWLEDGMENTS. We would like to thank Wendy Cooper, Alicia Holmes, and April Averill for purifying the enzymes used in this study; Jeffrey Blaisdel and Dr. Scott Kathe for determining the active fraction of the enzymes; and

Dr. Robert Hondal for helpful discussions. This research was supported by National Institutes of Health Grant P01 CA098993 and R01 CA090689 (to C.J.B.) awarded by the National Cancer Institute. Certain commercial equipment or materials are identified in this paper in order to specify adequately the experimental procedure. Such identification does not imply recommendation or endorsement by the National Institute of Standards and Technology, nor does it imply that the materials or equipment identified are necessarily the best available for the purpose.

- Wallace SS (2002) Biological consequences of free radical-damaged DNA bases. *Free Radic Biol Med* 33:1–14.
- David SS, O'Shea VL, Kundu S (2007) Base-excision repair of oxidative DNA damage. *Nature* 447:941–950.
- Hegde ML, Hazra TK, Mitra S (2008) Early steps in the DNA base excision/single-strand interruption repair pathway in mammalian cells. *Cell Res* 18:27–47.
- Eisen JA, Hanawalt PC (1999) A phylogenomic study of DNA repair genes, proteins, and processes. *Mutat Res* 435:171–213.
- Aravind L, Walker DR, Koonin EV (1999) Conserved domains in DNA repair proteins and evolution of repair systems. *Nucleic Acids Res* 27:1223–1242.
- Zharkov DO, Shoham G, Grollman AP (2003) Structural characterization of the Fpg family of DNA glycosylases. *DNA Repair* 2:839–862.
- Tchou J, et al. (1994) Substrate specificity of Fpg protein. Recognition and cleavage of oxidatively damaged DNA. *J Biol Chem* 269:15318–15324.
- Wallace SS, Bandaru V, Kathe SD, Bond JP (2003) The enigma of endonuclease VIII. *DNA Repair* 2:441–453.
- Bandaru V, Sunkara S, Wallace SS, Bond JP (2002) A novel human DNA glycosylase that removes oxidative DNA damage and is homologous to *Escherichia coli* endonuclease VIII. *DNA Repair* 1:517–529.
- Hazra TK, et al. (2002) Identification and characterization of a novel human DNA glycosylase for repair of cytosine-derived lesions. *J Biol Chem* 277:30417–30420.
- Hazra TK, et al. (2002) Identification and characterization of a human DNA glycosylase for repair of modified bases in oxidatively damaged DNA. *Proc Natl Acad Sci USA* 99:3523–3528.
- Morland I, et al. (2002) Human DNA glycosylases of the bacterial Fpg/MutM superfamily: An alternative pathway for the repair of 8-oxoguanine and other oxidation products in DNA. *Nucleic Acids Res* 30:4926–4936.
- Takao M, et al. (2002) A back-up glycosylase in Nth1 knock-out mice is a functional Nei (endonuclease VIII) homologue. *J Biol Chem* 277:42205–42213.
- Bandaru V, et al. (2007) Human endonuclease VIII-like (NEIL) proteins in the giant DNA Mimivirus. *DNA Repair* 6:1629–1641.
- Krokeide SZ, et al. (2009) Expression and purification of NEIL3, a human DNA glycosylase homolog. *Protein Expres Purif* 65:160–164.
- Takao M, et al. (2002) Novel nuclear and mitochondrial glycosylases revealed by disruption of the mouse Nth1 gene encoding an endonuclease III homolog for repair of thymine glycols. *EMBO J* 21:3486–3493.
- Toritsu K, Tsuchimoto D, Ohnishi Y, Nakabeppu Y (2005) Hematopoietic tissue-specific expression of mouse Neil3 for endonuclease VIII-like protein. *J Biochem-Tokyo* 138:763–772.
- Takao M, et al. (2009) Human Nei-like protein NEIL3 has AP lyase activity specific for single-stranded DNA and confers oxidative stress resistance in *Escherichia coli* mutant. *Genes Cells* 14:261–270.
- Dou H, Mitra S, Hazra TK (2003) Repair of Oxidized Bases in DNA Bubble Structures by Human DNA Glycosylases NEIL1 and NEIL2. *J Biol Chem* 278:49679–49684.
- Dou H, et al. (2008) Interaction of the human DNA glycosylase NEIL1 with proliferating cell nuclear antigen. The potential for replication-associated repair of oxidized bases in mammalian genomes. *J Biol Chem* 283:3130–3140.
- Kathe SD, et al. (2009) Plant and fungal Fpg homologs are formamidopyrimidine DNA glycosylases but not 8-oxoguanine DNA glycosylases. *DNA Repair* 8(5):643–653.
- Guo Y, et al. (2010) The oxidative DNA glycosylases of *Mycobacterium tuberculosis* exhibit different substrate preferences from their *Escherichia coli* counterparts. *DNA Repair(Amst)* 9(2):177–190.
- Krishnamurthy N, Muller JG, Burrows CJ, David SS (2007) Unusual structural features of hydantoin lesions translate into efficient recognition by *Escherichia coli* Fpg. *Biochemistry* 46:9355–9365.
- Hazra TK, et al. (2001) Repair of hydantoins, one electron oxidation product of 8-oxoguanine, by DNA glycosylases of *Escherichia coli*. *Nucleic Acids Res* 29:1967–1974.
- Krishnamurthy N, Zhao X, Burrows CJ, David SS (2008) Superior removal of hydantoin lesions relative to other oxidized bases by the human DNA glycosylase hNEIL1. *Biochemistry* 47:7137–7146.
- Fromme JC, Banerjee A, Verdine GL (2004) DNA glycosylase recognition and catalysis. *Curr Opin Struct Biol* 14:43–49.
- Hitomi K, Iwai S, Tainer JA (2007) The intricate structural chemistry of base excision repair machinery: Implications for DNA damage recognition, removal, and repair. *DNA Repair* 6:410–428.
- Das S, et al. (2007) Stimulation of NEIL2-mediated oxidized base excision repair via YB-1 interaction during oxidative stress. *J Biol Chem* 282:28474–28484.
- Blaisdell JO, Hatahet Z, Wallace SS (1999) A novel role for *Escherichia coli* endonuclease VIII in prevention of spontaneous G → T transversions. *J Bacteriol* 181:6396–6402.
- Dizdaroglu M, Kirkali G, Jaruga P (2008) Formamidopyrimidines in DNA: Mechanisms of formation, repair, and biological effects. *Free Radical Bio Med* 45:1610–1621.
- Kalam MA, et al. (2006) Genetic effects of oxidative DNA damages: Comparative mutagenesis of the imidazole ring-opened formamidopyrimidines (Fapy lesions) and 8-oxo-purines in simian kidney cells. *Nucleic Acids Res* 34:2305–2315.
- Patro JN, et al. (2007) Studies on the replication of the ring opened formamidopyrimidine, FapydG in *E. coli*. *Biochemistry* 46:10202–10212.
- Henderson PT, et al. (2003) The hydantoin lesions formed from oxidation of 7,8-dihydro-8-oxoguanine are potent sources of replication errors in vivo. *Biochemistry* 42:9257–9262.
- Kornyushyna O, Burrows CJ (2003) Effect of the oxidized guanine lesions spiroiminodihydantoin and guanidinohydantoin on proofreading by *Escherichia coli* DNA polymerase I (Klenow fragment) in different sequence contexts. *Biochemistry* 42:13008–13018.
- Hailer MK, Slade PG, Martin BD, Sugden KD (2005) Nei deficient *Escherichia coli* are sensitive to chromate and accumulate the oxidized guanine lesion spiroiminodihydantoin. *Chem Res Toxicol* 18:1378–1383.
- Henderson PT, et al. (2005) Urea lesion formation in DNA as a consequence of 7,8-dihydro-8-oxoguanine oxidation and hydrolysis provides a potent source of point mutations. *Chem Res Toxicol* 18:12–18.
- Duarte V, Gasparutto D, Jaquinod M, Cadet J (2000) In vitro DNA synthesis opposite oxazolone and repair of this DNA damage using modified oligonucleotides. *Nucleic Acids Res* 28:1555–1563.
- Duarte V, et al. (2001) Repair and mutagenic potential of oxaluric acid, a major product of singlet oxygen-mediated oxidation of 8-oxo-7,8-dihydroguanine. *Chem Res Toxicol* 14:46–53.
- Gasparutto D, et al. (1999) Synthesis and biochemical properties of cyanuric acid nucleoside-containing DNA oligomers. *Chem Res Toxicol* 12:630–638.
- Rolseth V, et al. (2008) Widespread distribution of DNA glycosylases removing oxidative DNA lesions in human and rodent brains. *DNA Repair* 7:1578–1588.
- Kauffmann A, et al. (2008) High expression of DNA repair pathways is associated with metastasis in melanoma patients. *Oncogene* 27:565–573.
- Hildrestrand GA, et al. (2009) Expression patterns of Neil3 during embryonic brain development and neoplasia. *BMC Neurosci* 10:45–53.
- Blaisdell JO, Wallace SS (2007) Rapid determination of the active fraction of DNA repair glycosylases: A novel fluorescence assay for trapped intermediates. *Nucleic Acids Res* 35:1601–1611.
- Dizdaroglu M, Bauche C, Rodriguez H, Laval J (2000) Novel substrates of *Escherichia coli* Nth protein and its kinetics for excision of modified bases from DNA damaged by free radicals. *Biochemistry* 39:5586–5592.
- Jaruga P, Kirkali G, Dizdaroglu M (2008) Measurement of formamidopyrimidines in DNA. *Free Radical Biol Med* 45:1601–1609.